Triggering and enhancing chaos with a prescribed target Lyapunov exponent using optimized perturbations of minimum power

C. Y. Soong[1,*] and W. T. Huang[2]
[1]*Department of Aerospace and Systems Engineering, Feng Chia University, Seatwen, Taichung, Taiwan 40724, Republic of China*
[2]*Department of Marine Mechanical Engineering, Chinese Naval Academy, Zuoying, Kaohsiung, Taiwan 81300, Republic of China*

(Received 25 August 2006; published 13 March 2007)

The objective of the present work is to propose a method for nonfeedback anticontrol of chaos with perturbations of minimum power for a preset control goal. The noted Lorenz system is employed as the test model for chaotification with the target state specified by a prescribed positive value of the largest Lyapunov exponent (LLE), $\tilde{\lambda}>0$. Periodic and quasiperiodic perturbations are used as control signals, and the signals parameters are optimized using a genetic algorithm under restriction of minimum power. Performance of the optimized signals in triggering chaos at an ordered state, fixed point or periodic, as well as further enhancing chaoticity at a chaotic state is explored. The present numerical experiments reveal the following interesting physics about chaotification. In general, the power for chaotification increases with the preset value of $\tilde{\lambda}$ and quasiperiodic signals can achieve the control goal with a lower power than periodic ones. Given the same increment of LLE from that of the uncontrolled state ($\lambda_{1,0}$), i.e., $\Delta\lambda=\tilde{\lambda}-\lambda_{1,0}$, the further enhancement of chaoticity in a chaotic state needs a higher control power than the triggering of chaos from an ordered state. The minimum power required for chaotification of an ordered state increases relatively slowly for lower $\tilde{\lambda}$ but increases drastically as the preset target LLE reaches a certain critical value. Most strikingly, the numerical experiments demonstrate that this critical value of $\tilde{\lambda}$ corresponds to LLE of the nearest chaotic state in the neighborhood of the uncontrolled state. Robustness of applying the present method in the presence of external noise is also demonstrated.

DOI: 10.1103/PhysRevE.75.036206 PACS number(s): 05.45.Gg, 05.45.Pq, 02.60.Pn, 87.23.Kg

I. INTRODUCTION

Chaotic behavior is usually detrimental to the performance of a dynamical system; therefore, numerous studies have been performed in order to suppress chaos and lead the dynamical system under control into an ordered state. However, there are a number of situations in which chaotification is both advantageous and desirable, for example, pulse combustion [1] and secure communication [2]. More recently, chaotic mixing in microfluidics [3] involving highly stable laminar flows has attracted a great deal of attention. These considerations provide strong motivation for recent investigations on chaotification of nonlinear systems. In the literature, the triggering of chaos in an ordered state or the enhancement of the existing chaoticity of a system is generally referred to as *anticontrol of chaos* or *chaotification*.

A number of methods for anticontrol of chaos have been realized by applying feedback schemes to systems with the state variables accessible during the system evolution. Yang *et al.* [4] proposed a method to sustain chaos in low-dimensional maps where only chaotic transients exist, and the concept was experimentally verified on a magneto-mechanical ribbon system [5]. Feedback control of chaotic saddles in two-dimensional maps to convert transient chaos into sustained chaos has been reported [6]. The global topology of the basin boundary saddle manifold structure can be used to design parameter control algorithms for sustaining chaos in parameter regimes where a crisis occurs [7,8]. The application of maintaining chaos in a high-dimensional system was developed [9]. Tsubone and Saito [10] proposed an occasional proportional feedback method that causes chaotification of a piecewise-linear circuit, and then verified the results through experimental implementations [11]. Chaotification of discrete-time systems has also been studied [12–14]. A similar case of chaotifying a continuous-time system by time-delay feedback control has also been investigated [15]. Chen *et al.* [16] studied anticontrol of chaos applying periodically impulsive inputs on a continuous time system. Konishi [17] proposed a feedback controller for generating chaos in an autonomous system. A piecewise-linear controller for chaos generation was proposed and applied in chaos generation [18–20]. Recently, feedback control was applied to the anticontrol of chaos in a rigid body system [21].

In applications of feedback control schemes it is generally necessary to measure the system state variables, thereby generating a control signal that is then applied to the signal to an accessible system parameter. In practice, it is relatively difficult to implement this class of schemes to some high-speed systems such as chaotic circuits and fast optoelectrical systems. Compared to feedback control techniques for inducing and enhancing chaotic behavior of nonlinear systems of small time scales, nonfeedback methods have the advantages of speed and flexibility. Furthermore, on-line monitoring and processing are not required. Of course, in order to find appropriate signals for control, the nature of the system dynamics must be understood *a priori*. This class of control approaches is suitable for cases in which no real-time data or

*Corresponding author. Electronic address: cysoong@fcu.edu.tw

only highly limited measurements of the system state are available. A number of studies on nonfeedback anticontrol of chaos have been carried out with various control signals, for example, constant perturbations [22,23], weak noise signals [24,25], and weak periodic perturbations [26–28]. A few studies have also demonstrated the dual function of suppressing and inducing chaos with applications of weak periodic perturbations to the nonlinear dynamic systems [29,30].

The nonfeedback methods proposed in literature used control signals that had been assigned somewhat intuitively or arbitrarily rather than sought out based on optimization of the signal parameters. In the case of using a periodic perturbation as the control signal, with the frequency fixed *a priori*, the amplitude for achieving the control goal can be found by simply varying its value within a range. The signal determined in this manner is not optimal in any sense. Additionally, for a multiparameter control signal, the method for determining the proper combination of the parameter values is a problem. The approach used in finding a signal able to work efficiently in achieving a preset control target seems significant and this motivates the present study.

The objective of the present work is to propose a method for nonfeedback anticontrol of chaos with perturbations of minimum power for a preset control goal. With this methodology, we can define the control target of a chaotic state with a prescribed positive value of the largest Lyapunov exponent (LLE), $\tilde{\lambda}>0$. Periodic perturbations of single frequency with high harmonics as well as quasiperiodic signals of multiple noncommensurate frequencies are considered and then tested on a nonlinear continuous time system, i.e., the Lorenz system. The signals are of minimum power with parameters found by an optimization procedure based on a genetic algorithm (GA) originally proposed for chaos suppression [31,32]. This GA is chosen as the optimization approach since it has better global searching when compared with calculus-based methods such as steepest descent technique. The method can be implemented to trigger chaos in parametric regions of ordered states, either fixed-point or periodic, and to enhance chaoticity of systems in a chaotic state. The effectiveness of chaos triggering and enhancement is investigated, as is switching control between ordered and chaotic states. The robustness of the present method's application in the presence of external noise is also investigated.

II. OPTIMIZATION OF SIGNALS FOR ANTICONTROL OF CHAOS

A. Control signals

Weak perturbations in the form of finite Fourier series of N modes have a general form as follows:

$$u(t)=\sum_{n=1}^{N}[a_n\cos(\omega_n t+\varphi_n)+b_n\sin(\omega_n t+\varphi_n)], \qquad (1)$$

where the parameters a_n and b_n are the amplitudes, ω_n the frequency, and φ_n the phase shift of the nth mode. In general, the ratio of two modes, ω_j/ω_k, is not integer. A signal with multiple *noncommensurate* frequencies as mentioned above is defined as a quasiperiodic signal. For $\omega_n=n\omega$ and $\varphi_n=\varphi$, the signal is expressed in the form of

$$u(t)=\sum_{n=1}^{N}[a_n\cos(n\omega t+\varphi)+b_n\sin(n\omega t+\varphi)], \qquad (2)$$

which is a periodic signal of frequency ω with higher harmonic modes $n\omega$. The power of the control signal, both periodic and quasiperiodic, can be defined in terms of the amplitudes, viz.,

$$P=\frac{1}{2}\sum_{n=1}^{N}(a_n^2+b_n^2). \qquad (3)$$

B. Optimization of the control signals

In the present GA-based method, the amplitudes a_n and b_n, the frequencies ω_n (or ω) and the phase angles φ_n (or φ) play the role of gene to form the chromosome or individual, and the values of the parameters are optimized towards the maximum fitness by using the GA. Each member of the current population is evaluated by a fitness function defined *a priori* and the value assigns each individual a probability of being reproduced as a member in next generation. The GA used to optimize the control signals is described below.

To evaluate the performance or appropriateness of the individuals in the GA procedure, a fitness function, f, proposed previously [31] is applied. It is defined based on the consideration of minimum power of the control signal and closeness of the controlling state to the target characterized by the largest Lyapunov exponent, *viz.*,

$$f=\frac{1}{\Delta\lambda^*+P^*}, \qquad (4)$$

where $\Delta\lambda^*=|\lambda-\tilde{\lambda}|/\max|\lambda-\tilde{\lambda}|$, $P^*=P/P_m$, and λ and $\tilde{\lambda}$ are the current and prescribed target values of the LLE of the system state, P stands for the power of the signal and P_m for the maximum power in the current population. The function f is maximized as $\Delta\lambda^*$ and P^* approach minimum values. The LLE can be determined by using the algorithm proposed in Ref. [33]. For the system at a regular state, the target LLE $\tilde{\lambda}$ can be set as a positive value for the final state of chaotic motion, while for an existing chaotic state, the value of the target $\tilde{\lambda}$ can be set higher to enhance the chaoticity in system behavior.

The GA evolution used in the present work consists of the procedures of proportionate or roulette wheel selection, arithmetic crossover, nonuniform mutation and elitism strategy. The operators of crossover and mutation are applied to the intermediate population to generate new offspring. Then each member of the offspring is evaluated by calculating its fitness function. To improve the convergence rate, an elitism strategy is employed, i.e., 50% of the individuals with higher fitness values are selected from the pool of the parents as well as the offspring to form a new population. The iteration continues until the best individual is found. Evolution with a large population usually needs more time to converge, but

TABLE I. System states simulated and the neighboring (nearest) chaotic state of each case described by the system parameter R and the largest Lyapunov exponent (λ).

	System state simulated			Nearest chaotic state	
State No. (J)	R	$\lambda_{1,0}$ (LLE)	Attractor[a]	R_{nc}	λ_{nc} (LLE)
1	20	−0.1548	FP	24.7	0.740
2	160	$2\times10^{-4}\approx0$	P	166.6	1.697
3	28	0.906	SA		
4	100	$-6\times10^{-4}\approx0$	P	101.32	1.5076

[a]FP, fixed point; P, periodic; SA, strange attractor (chaotic state).

that with a small population size may not converge to a satisfactory result. According to our previous experiences, a population size of $N_p=200$ with a crossover parameter $p_c=0.7$ and a mutation probability $p_m=0.4$ is appropriate. More detailed description of the GA procedure and the other parameters employed in the GA evolution can be found in our previous work [31].

The GA evolution for optimization of the control signals terminates when the preset stopping criterion, $|\lambda_b-\tilde{\lambda}|/|\tilde{\lambda}|<\varepsilon$, is met, where the parameter λ_b denotes the LLE of the best individual in the current population, and ε is a prescribed tolerance. In the present work, tests on a couple of cases and the results thereof revealed that the powers of the signals found with tolerances of $\varepsilon=10^{-2}$ and 10^{-3} were very close. Therefore in order to save computational time for simulation, this study uses a tolerance of $\varepsilon=10^{-2}$.

III. TEST MODEL

In this section, we present a series of numerical experiments to demonstrate the effectiveness of the proposed method under various conditions. A noted three-mode nonlinear dynamical system, the Lorenz system [34] for atmospheric convection flow, is considered as the test model. Considering control via parameter modulation, the major system parameter R can be expressed as $R=R_0[1+u(t)]$ with $u(t)$ denoting the control signal, i.e.,

$$\dot{x}=\Pr(y-x),\quad \dot{y}=-xz+R_0[1+u(t)]x-y,$$

$$\dot{z}=xy-bz. \tag{5}$$

The parameters in the present GA method are set as follows: the genes of chromosomes are encoded by using floating-point numbers. To designate control signals of different modes at various conditions, the notation $F_{I,J}^{P}-K$ is used for periodic signals of harmonic modes and $F_{I,J}^{Q}-K$ for quasiperiodic signals of multiple frequencies, where the subscript I is the mode number and the subscript J is an index for denoting states at different values of R. The integer K designates various signals with the same values of I and J. The simulations are performed with a C-language code based on the fourth-order Runge-Kutta integration scheme.

In this study, the system parameters Pr (where Pr is the Prandtl number) and b are fixed as $\Pr=10$ and $b=8/3$ through the whole analysis. Table I lists four states, showing their system parameter R and largest Lyapunov exponent $\lambda_{1,0}$. The table also shows the neighboring chaotic state of each case, as characterized by the system parameter R_{nc} and the LLE λ_{nc}. The first three cases are the fixed point (FP) state at $R=20$, the periodic (P) state at $R=160$, and the chaotic state or strange attractor (SA) at $R=28$. In Lorenz system dynamics, there are numerous periodic windows along the variation of system parameter R, and so one more periodic state at $R=100$ is included in the analysis of minimum power required.

IV. RESULTS AND DISCUSSION

A. Anticontrol of chaos with periodic perturbation signals

The fixed-point state at $R=20$ (denoted by $J=1$) and the periodic attractor at $R=160$ (denoted by $J=2$) are considered for study in the triggering of chaos. The value of LLE at the originally uncontrolled states $R=20$ and $R=160$ are $\lambda_{1,0}=-0.1548$ and $\lambda_{1,0}=2\times10^{-4}\approx0$, respectively. The performance of applying GA-optimized weak perturbations for anticontrol of chaos is investigated. It is noted that at $R=20$, the single-point phase diagram and the blank spectrum for the fixed-point attractor are trivial. By applying a GA-optimized weak perturbation $F_{2,1}^{P}-1$ ($P=2.31\times10^{-4}$) found for the target LLE $\tilde{\lambda}=0.1$, the system behavior turns into a chaotic one. Similarly at $R=160$, the uncontrolled Lorenz system lies at a periodic state shown in Fig. 1(a) can be chaotified by applying the optimized low-power signal, $F_{2,2}^{P}-1$ ($P=1.11\times10^{-6}$).

The procedures of the optimized signals and the simulation can be addressed by using the case of $R=160$ as a typical example. From the data of the uncontrolled state in Fig. 1(a), it is found that the relatively strong energy-contained modes are of frequencies $\omega=5.36$ and 15.96. The perturbation frequency and phase shift of the initial individuals are set in the ranges of $\omega\in[15.0,19.0]$ and $\varphi\in[-\pi,\pi]$. In addition, since the optimization procedure may not converge with too small a range of amplitudes a_i and b_i, the amplitudes of the initial individuals are specified in an interval of $[0,5\times10^{-3}]$. The integrations are performed within the time period $t\in[0,500]$ with a time step $\Delta t=5\times10^{-3}$ and an initial condition $(x_0,y_0,z_0)=(0.1,0.1,0.1)$. The control signal is applied to the system at the time instant $t=50$. The control target is set to be a chaotic state with a specified LLE, say $\tilde{\lambda}=0.1$. A larger value of $\tilde{\lambda}$ corresponding to a higher level of

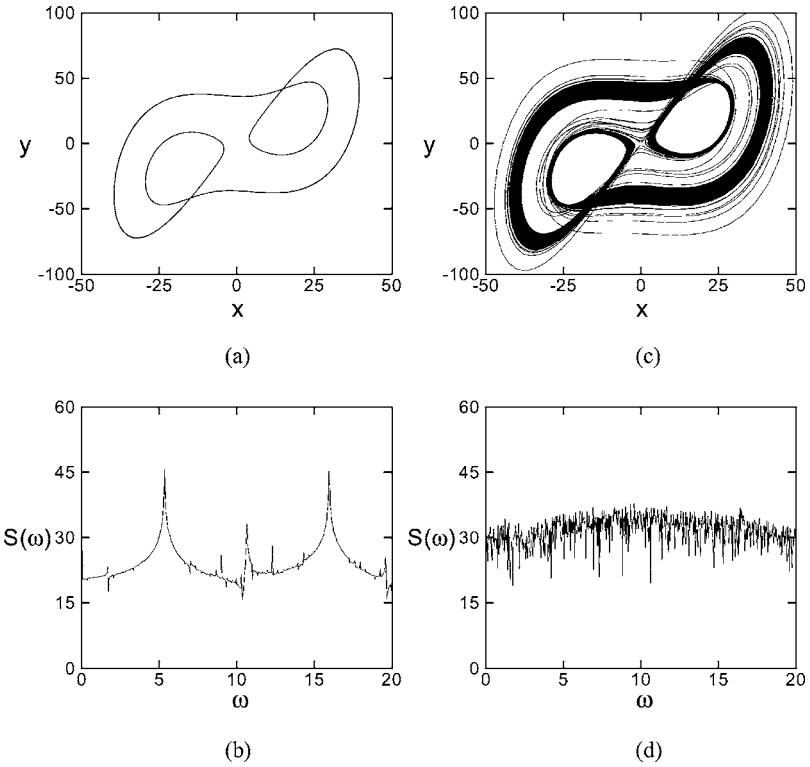

FIG. 1. (a) The phase diagram on the xy plane and (b) the spectrum of the Lorenz system at uncontrolled periodic state of Pr=10, $b=8/3$, and $R=160$. The resultant chaotic state of LLE $\tilde{\lambda}=0.1$ after applying the control signal $F_{2,2}^{P}-1$ is designated by the corresponding (a) phase diagram and (b) spectrum.

chaoticity usually leads to a signal of higher power.

The optimized signals of various modes determined by the present approach for $R=20$ are shown in Table II. The data reveal that the power of the control signals found by the present method are quite low. The power is not necessarily reduced with additional Fourier modes. Furthermore, in a similar result as the performance in suppressing chaos [31,32], the results also demonstrated that the GA-based method is very effective and 2-mode signals seem quite appropriate from the perspective of low power and simplicity. In practical applications, it is beneficial in saving computation costs. As an illustrative example, Fig. 1 shows that the present GA-optimized signals of extremely low power effectively destabilize the periodic state at $R=160$.

TABLE II. The amplitudes, frequencies, phases and powers of optimized periodic perturbation signals of harmonic modes for anticontrol of the Lorenz system at $R=20$.

Signal	Amplitude, frequency and phase	Power (Target state)
$F_{1,1}^{P}-1$	$a_1=0.01409400$; $b_1=0.01849650$	$P=2.70\times10^{-4}$
	$\omega=8.10110000$; $\varphi=-2.85644565$	(SA, $\tilde{\lambda}=0.1$)
$F_{2,1}^{P}-1$	$a_1=0.00056323$; $b_1=0.01969174$	$P=2.31\times10^{-4}$
	$a_2=0.00027923$; $b_2=0.00863233$	(SA, $\tilde{\lambda}=0.1$)
	$\omega=8.08435065$; $\varphi=-2.97670011$	
$F_{3,1}^{P}-1$	$a_1=0.01852897$; $b_1=0.01047457$	$P=2.46\times10^{-4}$
	$a_2=0.00515417$; $b_2=0.00201504$	(SA, $\tilde{\lambda}=0.1$)
	$a_3=0.00301954$; $b_3=0.00016828$	
	$\omega=8.09187666$; $\varphi=2.95501125$	
$F_{4,1}^{P}-1$	$a_1=0.01894770$; $b_1=0.01121813$	$P=2.49\times10^{-4}$
	$a_2=0.00149047$; $b_2=0.00175995$	(SA, $\tilde{\lambda}=0.1$)
	$a_3=0.00031107$; $b_3=0.00060468$	
	$a_4=0.00100617$; $b_4=0.00255947$	
	$\omega=8.08375543$; $\varphi=-3.10609291$	
$F_{5,1}^{P}-1$	$a_1=0.01880835$; $b_1=0.01682818$	$P=3.35\times10^{-4}$
	$a_2=0.00153102$; $b_2=0.00051326$	(SA, $\tilde{\lambda}=0.1$)
	$a_3=0.00146064$; $b_3=0.00082813$	
	$a_4=0.00342857$; $b_4=0.00367725$	
	$a_5=0.00111160$; $b_5=0.00040954$	
	$\omega=8.13261557$; $\varphi=-2.91623735$	

To further check the present chaotification method with perturbation signal optimization, we also perform the numerical experiments with the signal frequency ω given *a priori* but the amplitudes and phase shifts of the signals optimized by GA. For chaotification of the periodic state at $R=160$ with a 2-mode periodic model, Fig. 2 presents the correlation of the minimum control power required versus the preset value of the frequency. After a series of 20 simulations (scanning ω from 1 to 20) with five parameters to be determined, it is found that the lowest power required is $P\approx1\times10^{-6}$ at an ω around 18. Optimizing all six signal parameters generates a signal $F_{2,2}^{P}-1$ of frequency $\omega=18.630\,809\,13$ and power $P=1.11\times10^{-6}$ (in Table III), which is very close to that mentioned above but needs a significantly shorter searching time. This fact demonstrates the effectiveness of the present optimization procedure.

In the previous nonfeedback methods, the proper control signal was found by scanning one specific parameter. In a work concerned with the control of the Lorenz system [35], Gaussian noise in the form of $D\eta(t)$ was added to each of the equations and employed as the control signal for chaotification. They varied the signal strength D from a small value (0.001) and found that, at a state around $R=24$, the system

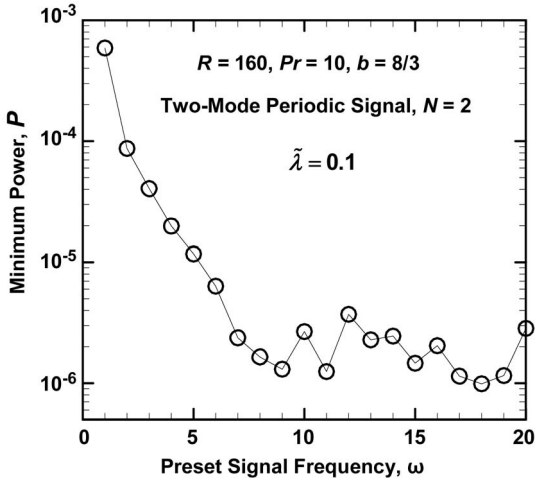

FIG. 2. Minimum control power correlation with the signal frequency under the conditions of $R=160$, Pr$=10$, $b=8/3$ with the target LLE, $\tilde{\lambda}=0.1$. The control signals employed are of two-mode ($N=2$) and periodic with the signal frequency preset.

behavior turns chaotic as the parameter D is raised up to the value of 0.2 or the power $P=2\times10^{-2}$ ($P\equiv D^2/2$). In a similar situation, using our GA-optimized perturbation under the restriction of minimum power to chaotify the state at $R=24$ to the target of $\tilde{\lambda}=0.1$, the required signal power is only $P=5.632\times10^{-7}$. Obviously, the present method of GA optimization has the merit of attaining the appropriate control signal to achieve the control goal under a specified restriction.

In order to demonstrate further enhancing the chaoticity of a chaotic system, the Lorenz system at $R=28$ (denoted by $J=3$) with the LLE $\lambda_{1,0}=0.906$ and the LLE of the target state $\tilde{\lambda}=1.5$ is considered. The perturbation signal $F^P_{2,3}-1$ of $P=5.14\times10^{-3}$ is found and employed in the simulation. The present control strategy can achieve the specified level of chaos by presetting a desired LLE of the control target, $\tilde{\lambda}$.

B. Anticontrol of chaos with quasiperiodic perturbation signals

In this section, anticontrol of chaos by using quasiperiodic signals is explored. The control signal consists of multiple noncommensurate frequencies. The signal parameters are sought by GA-based optimization towards maximum fitness. From the present simulations, it was found that in general, the power of the GA-optimized quasiperiodic signals is even lower than the periodic signal of the same number of modes. For example, the controlling power of the signal $F^Q_{2,1}-1$ is only 36.2% of the signal $F^P_{2,1}-1$. In addition, it is seen that the power of quasiperiodic signals slightly decreases with an increase in the number of modes, though the powers are of the same order. Figure 3 presents an example of chaotification of the fixed-point state at $R=20$ by applying an optimized quasiperiodic signal. Initially, the system is brought to a fixed-point state at $R=20$ at the time instant $t=30$ and then, at $t=50$, the quasiperiodic signal $F^Q_{2,1}-1$ is applied. The system is chaotified with the time series and power spectrum shown in Fig. 3.

TABLE III. The amplitudes, frequencies, phases and powers of optimized periodic perturbation signals of two harmonic modes for anticontrol of the Lorenz system.

Signal	Amplitude, frequency and phase	Power (Target state)
$F^P_{2,1}-2$	$a_1=0.00143764$; $b_1=0.02550090$	$P=3.42\times10^{-4}$
	$a_2=0.00517612$; $b_2=0.00219985$	(Chaos, $\tilde{\lambda}=0.5$)
	$\omega=7.98582994$; $\varphi=1.23867537$	
$F^P_{2,1}-3$	$a_1=0.03844844$; $b_1=0.00095879$	$P=8.20\times10^{-4}$
	$a_2=0.00365806$; $b_2=0.01215993$	(SA, $\tilde{\lambda}=0.75$)
	$\omega=7.83274335$; $\varphi=0.35609177$	
$F^P_{2,1}-4$	$a_1=0.00163317$; $b_1=0.00500134$	$P=1.98\times10^{-5}$
	$a_2=0.00091720$; $b_2=0.00332062$	(P-1, $\tilde{\lambda}=0$)
	$\omega=8.51275713$; $\varphi=2.75576785$	
$F^P_{2,1}-5$	$a_1=0.00129526$; $b_1=0.00015212$	$P=8.98\times10^{-7}$
	$a_2=0.00029457$; $b_2=0.00009077$	(P-1, $\tilde{\lambda}=-0.15$)
	$\omega=8.69950751$; $\varphi=-2.72441691$	
$F^P_{2,2}-1$	$a_1=0.00001430$; $b_1=0.00130940$	$P=1.11\times10^{-6}$
	$a_2=0.00001545$; $b_2=0.00070668$	(SA, $\tilde{\lambda}=0.1$)
	$\omega=18.63080913$; $\varphi=-1.76149793$	
$F^P_{2,2}-2$	$a_1=0.00358462$; $b_1=0.00088352$	$P=6.82\times10^{-6}$
	$a_2=0.00008091$; $b_2=0.00002439$	(SA, $\tilde{\lambda}=2.0$)
	$\omega=18.95210579$; $\varphi=2.57769180$	
$F^P_{2,2}-3$	$a_1=0.00135269$; $b_1=0.00037122$	$P=1.16\times10^{-6}$
	$a_2=0.00057204$; $b_2=0.00015552$	(SA, $\tilde{\lambda}=0.5$)
	$\omega=18.54721313$; $\varphi=-2.83780196$	
$F^P_{2,2}-4$	$a_1=0.00055599$; $b_1=0.00107361$	$P=1.44\times10^{-6}$
	$a_2=0.00072216$; $b_2=0.00094739$	(SA, $\tilde{\lambda}=1.0$)
	$\omega=17.61008734$; $\varphi=-1.55830369$	
$F^P_{2,2}-5$	$a_1=0.00056057$; $b_1=0.00143612$	$P=3.45\times10^{-6}$
	$a_2=0.00192868$; $b_2=0.00089087$	(P-15, $\tilde{\lambda}=-0.1$)
	$\omega=17.42733980$; $\varphi=3.07295689$	
$F^P_{2,2}-6$	$a_1=0.00025313$; $b_1=0.00156317$	$P=2.27\times10^{-6}$
	$a_2=0.00126755$; $b_2=0.00064794$	(P-6, $\tilde{\lambda}=-0.15$)
	$\omega=16.32067634$; $\varphi=3.10936150$	
$F^P_{2,3}-1$	$a_1=0.00005705$; $b_1=0.09830647$	$P=5.14\times10^{-3}$
	$a_2=0.00010337$; $b_2=0.00276817$	(SA, $\tilde{\lambda}=1.5$)
	$\omega=19.56588959$; $\varphi=2.98970451$	

C. Switching control

To demonstrate the ability of state switching by the optimized perturbation signals, switching control with a sequence of successive chaotification and stabilization on the Lorenz system at $R=20$ (fixed point) is performed. The sequential control for alternatively changing the system state is performed by employing periodic signals including the above mentioned $F^P_{2,1}-1$ ($\tilde{\lambda}=0.1$) and another four signals, $F^P_{2,1}-2$ ($\tilde{\lambda}=0.5$), $F^P_{2,1}-3$ ($\tilde{\lambda}=0.75$), $F^P_{2,1}-4$ ($\tilde{\lambda}=0$, for a period-1, or P-1 state), $F^P_{2,1}-5$ ($\tilde{\lambda}=-0.15$, P-1). The amplitudes, frequencies, phase shifts and powers of the above four signals are listed in Table III. The system lies initially at a

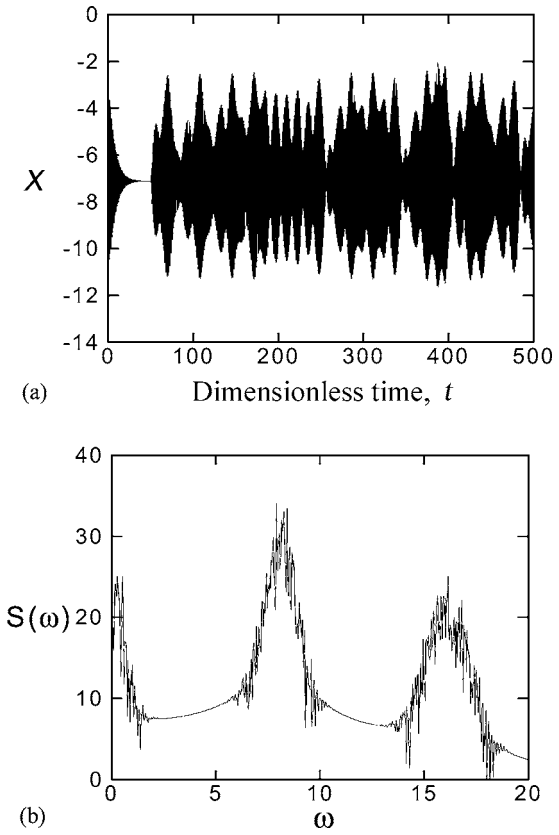

FIG. 3. The fixed-point attractor at Pr=10, $b=8/3$, and $R=20$ can be destabilized to a chaotic state by applying the control signal $F_{2,1}^{Q}-1$ optimized for $\tilde{\lambda}=0.1$, (a) the time series of x and (b) power spectrum.

fixed-point state until the signal $F_{2,1}^{P}-1$ is applied to the system at the time $t=1000$. Then the system state becomes strange attractor (SA) chaotic with LLE $\tilde{\lambda}=0.1$. At $t=2000$, the control signal is replaced by $F_{2,1}^{P}-4$ and thus the system is stabilized to a P-1 state. Subsequently, the system dynamics varies with the alternation of the control signals $F_{2,1}^{P}-2$, $F_{2,1}^{P}-5$, and $F_{2,1}^{P}-3$ every 1000 time units. Finally, at $t=6000$, the control signal is removed and the system returns to the original fixed-point state. The sequence of the switching control, FP→SA→P-1→SA→P-1→SA→FP, is illustrated in Fig. 4 with the state variable x of the Poincaré section $y=-7$ plotted versus time. Figure 5 shows the switching control of the Lorenz system at $R=160$ (periodic state) by alternately applying control signals $F_{2,2}^{P}-3$ ($\tilde{\lambda}=0.5$), $F_{2,2}^{P}-5$ ($\tilde{\lambda}=-0.1$, P-15), $F_{2,2}^{P}-4$ ($\tilde{\lambda}=1.0$), $F_{2,2}^{P}-6$ ($\tilde{\lambda}=-0.15$, P-6) and $F_{2,2}^{P}-2$ ($\tilde{\lambda}=2.0$) as listed in Table III. The switching sequence of this process is P-3→SA→P-15→SA→P-6→SA→P-3. The results shown in Figs. 4 and 5 demonstrate the robustness and effectiveness of the present approach used in switching control and anticontrol of chaos with signals optimized in a searching range around the resonant frequency.

Figure 6 is a demonstration of the switching control by using optimized quasiperiodic signals. The switching signals include the previous $F_{2,1}^{Q}-1$ ($\tilde{\lambda}=0.1$) and another four signals: $F_{2,1}^{Q}-2$ ($\tilde{\lambda}=0.5$), $F_{2,1}^{Q}-3$ ($\tilde{\lambda}=0.75$), $F_{2,1}^{Q}-4$ ($\tilde{\lambda}=-0.05$, P-1) and $F_{2,1}^{Q}-5$ ($\tilde{\lambda}=-0.1$, P-1). The amplitudes, frequencies, phase shifts and powers of the four signals above are listed in Table IV. The system is initially at a fixed-point state of $R=20$ until the signal $F_{2,1}^{Q}-1$ is applied to the system at the time instant $t=1000$. The system behavior shows a chaotic state of the LLE $\tilde{\lambda}=0.1$. At $t=2000$, the control signal changes to $F_{2,1}^{Q}-4$ and thus the system behavior is of a P-1 orbit. The control signal is sequentially changed to $F_{2,1}^{Q}-2$, $F_{2,1}^{Q}-5$, and $F_{2,1}^{Q}-3$ every 1000 time units. Finally, at $t=6000$, the control signal is removed and the system returns to the fixed-point state. This switching sequence FP→SA→P-1→SA→P-1→SA→FP is shown in Fig. 6 with the state variable x of the Poincaré section $y=-7$ plotted versus time.

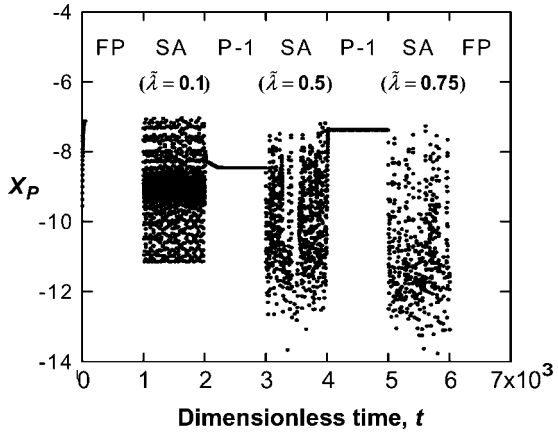

FIG. 4. Switching control of Lorenz system at Pr=10, $b=8/3$, and $R=20$. Control is activated in the time period $t=1000$ to $t=6000$ and sequentially switched signals $F_{2,1}^{P}-1$ ($\tilde{\lambda}=0.1$), $F_{2,1}^{P}-4$ ($\tilde{\lambda}=0$, P-1), $F_{2,1}^{P}-2$ ($\tilde{\lambda}=0.5$), $F_{2,1}^{P}-5$ ($\tilde{\lambda}=-0.15$, P-1), $F_{2,1}^{P}-3$ ($\tilde{\lambda}=0.75$) every 1000 time units.

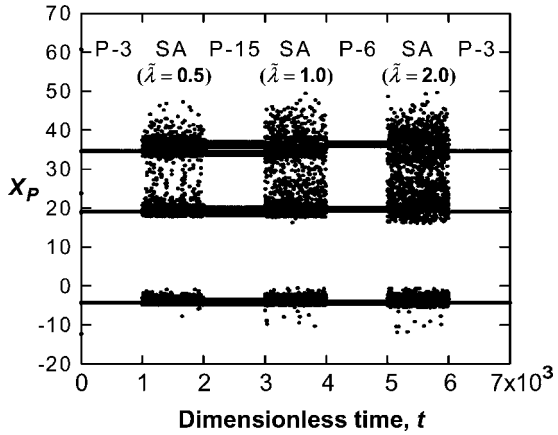

FIG. 5. Switching control of Lorenz system at Pr=10, $b=8/3$, and $R=160$. Control is activated in the time period $t=1000$ to $t=6000$ and sequentially switched signals $F_{2,2}^{P}-3$ ($\tilde{\lambda}=0.5$), $F_{2,2}^{P}-5$ ($\tilde{\lambda}=-0.1$, P-15), $F_{2,2}^{P}-4$ ($\tilde{\lambda}=1.0$), $F_{2,2}^{P}-6$ ($\tilde{\lambda}=-0.15$, P-6), and $F_{2,2}^{P}-2$ ($\tilde{\lambda}=2.0$) every 1000 time units.

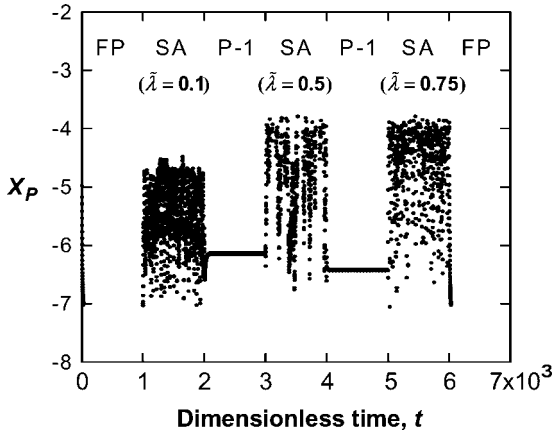

FIG. 6. Switching control of Lorenz system with Pr=10, $b=8/3$, and $R=20$. Control is activated in the time period $t=1000$ to $t=6000$ and sequentially switched signals $F^Q_{2,1}-1$ ($\tilde{\lambda}=0.1$), $F^Q_{2,1}-4$ ($\tilde{\lambda}=-0.05$, P-1), $F^Q_{2,1}-2$ ($\tilde{\lambda}=0.5$), $F^Q_{2,1}-5$ ($\tilde{\lambda}=-0.1$, P-1), $F^Q_{2,1}-3$ ($\tilde{\lambda}=0.75$) every 1000 time units.

D. Variation of power of genetic algorithm optimized signals with prescribed target largest Lyapunov exponent

To explore the influence of the preset control target on the power of the optimized signal, we use 2-mode ($N=2$) signals for anticontrol of chaos in the Lorenz system with the target $\tilde{\lambda} \sim O(10^{-2})$ to $O(1)$. Four uncontrolled states with the related data listed in Table I are studied. In Fig. 7(a), the powers of the optimized control signals are plotted versus the preset LLE $\tilde{\lambda}$ for the target state. It shows that, in general, the powers of the GA-optimized signals increase with an increase in the value of $\tilde{\lambda}$. This is reasonable since leading the system to a more chaotic state with a higher LLE requires a stronger signal.

For $R=20$, as $\tilde{\lambda}$ is raised over 0.7, the signal power required rises dramatically. It is interesting to note that the Lorenz system enters a chaotic regime at $R=24.7$ with the LLE around 0.74, which is the nearest chaotic state in the neighborhood of $R=20$. As the target value of $\tilde{\lambda}$ is far below the LLE of this nearest chaotic state, the applied weak perturbation simply perturbs the system towards a state of chaotic behavior by destabilizing the system via resonance with

TABLE IV. The amplitudes, frequencies, phases and powers of optimized two-mode quasiperiodic perturbation signals for anticontrol of the Lorenz system at $R=20$.

Signal	Amplitude, frequency and phase	Power (Target state)
$F^Q_{2,1}-1$	$a_1=0.00805496$, $b_1=0.00289911$	$P=8.37\times10^{-5}$
	$a_2=0.00955858$, $b_2=0.00166354$	(SA, $\tilde{\lambda}=0.1$)
	$\omega_1=7.89232154$, $\omega_2=8.38585304$	
	$\varphi_1=2.76843313$, $\varphi_2=1.76859132$	
$F^Q_{2,1}-2$	$a_1=0.01332743$; $b_1=0.00080929$	$P=1.55\times10^{-4}$
	$a_2=0.00842025$; $b_2=0.00775758$	(SA, $\tilde{\lambda}=0.5$)
	$\omega_1=7.52960518$; $\omega_2=8.28617950$	
	$\varphi_1=-2.03017694$; $\varphi_2=-1.37042605$	
$F^Q_{2,1}-3$	$a_1=0.00608584$; $b_1=0.04643994$	$P=1.10\times10^{-3}$
	$a_2=0.00028648$; $b_2=0.00005405$	(SA, $\tilde{\lambda}=0.75$)
	$\omega_1=7.85371980$; $\omega_2=8.47923787$	
	$\varphi_1=3.01448452$; $\varphi_2=-0.87394181$	
$F^Q_{2,1}-4$	$a_1=0.00023200$; $b_1=0.00020265$	$P=1.24\times10^{-5}$
	$a_2=0.00001331$; $b_2=0.00496459$	(P-1, $\tilde{\lambda}=-0.05$)
	$\omega_1=7.85672381$; $\omega_2=8.55283827$	
	$\varphi_1=-0.62476023$; $\varphi_2=0.99146064$	
$F^Q_{2,1}-5$	$a_1=0.00003696$; $b_1=0.00005075$	$P=5.69\times10^{-6}$
	$a_2=0.00096300$; $b_2=0.00323395$	(P-1, $\tilde{\lambda}=-0.1$)
	$\omega_1=8.49236738$; $\omega_2=8.61693953$	
	$\varphi_1=-0.74683038$; $\varphi_2=1.97524126$	

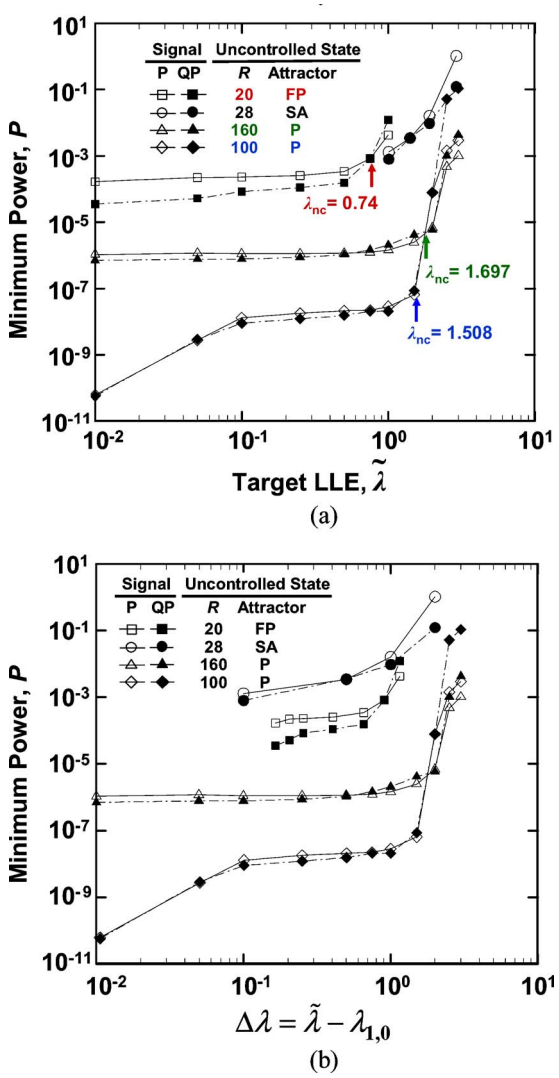

FIG. 7. (Color online) Powers of the GA-optimized periodic and quasiperiodic signals required for chaotification of the Lorenz system at $R=20$, 28, 100, and 160 with the influences of (a) the target LLE, $\tilde{\lambda}$; and (b) the differences between the LLEs of uncontrolled and the target states, $\Delta\lambda=\tilde{\lambda}-\lambda_{1,0}$. Signal: P, periodic; QP, quasiperiodic. Attractors: FP, fixed point; SA, strange attractor; P, periodic.

one of the modes at its original state and the power required can be lowered. Increasing the value of the preset target LLE $\tilde{\lambda}$ simply implies more profound chaotification and the power of the signal required for chaotification of the system increases gradually until $\tilde{\lambda}$ approaches that of the nearest chaotic state, 0.74. With a value beyond this one, the system is not only disturbed to a chaotic state but also to one of excess chaoticity and, therefore, the power needed to achieve this control goal increases drastically.

For the case of the periodic state of $R=160$, the abrupt rise of the required control power in the region of $\tilde{\lambda}$ between 1 and 2 can be observed. From Table I, it is observed that the nearest chaotic state immediately out of the periodic window, $145 \leq R \leq 166$, is $R=166.6$ with corresponding LLE$=1.697$. This result demonstrates that the power of the optimal perturbation abruptly increases as the value of the target LLE $\tilde{\lambda}$ reaches 1.7. Similarly this behavior is also found in the case of $R=100$, for which $\lambda_{1,0}=1.5076$ and obviously, the minimum control power required increases drastically at $\tilde{\lambda} \approx 1.5$.

It is found from the correlation of GA-optimized control power versus target LLE in Fig. 7(a) that the destabilization and chaotification of ordered states ($R=20$, 100, and 160) are characterized by a region of slow-varying power followed by fast growth. However, the case of enhancing chaoticity of a chaotic state shows a different trend. To address this point, the ascending trend of the required control power with the preset target LLE for the chaotic state $R=28$ is also examined. However, there is no slow-varying region in the correlation of the minimum power versus the target LLE. Further increasing the chaoticity of a chaotic state needs more power just like that described above.

By comparing the performance of the periodic and quasiperiodic signals, we found that these two kinds of GA-optimized signals have quite similar trends in variation of power with LLE. However, for the cases of chaotifying an ordered state, e.g., $R=20$, 100 or 160, the quasiperiodic signals generally perform more efficiently since they need relatively lower power to achieve the control goal. For higher values of the prescribed target LLE, the quasiperiodic signals may need relatively higher powers than periodic signals to reach the control goal. At $R=28$, the present results show that quasiperiodic signals need slightly lower control power to further enhance the chaoticity of the original state. Plots of power of the optimized signals versus $\Delta\lambda=\tilde{\lambda}-\lambda_{1,0}$ (the difference between the LLE of the target, $\tilde{\lambda}$ and that of the originally uncontrolled state, $\lambda_{1,0}$) are shown in Fig. 7(b). The data reveal that, for chaotification based on the same increment in the system LLE $\Delta\lambda$, the control power needed for enhancement of chaoticity in the chaotic state is highest, that needed for chaotification of the periodic state is lowest, and that needed for the fixed-point state is somewhere in between.

E. Chaotification with the presence of background noise

To examine the robustness of the present method of anticontrol of chaos, the signals found by GA under noise-free conditions are used to perform chaotification at various states. A white Gaussian noise of strength σ is added to the right-hand side of each of the three equations simultaneously. For small noise, the method performs well. Here we consider external noise of strength in the range of $10^{-6} \leq \sigma \leq 1$. In Fig. 8(a), for inducing chaos at a fixed-point state, $R=20$, the variation of LLE of the achieved state with the noise strength σ is presented. The GA-optimized control signal $F_{2,1}^{P}-1$ with the power $P=2.31\times10^{-4}$ for the target $\tilde{\lambda}=0.1$ is applied. Clearly, the final state drifts a little in the presence of the external noise. However, in this case, the anticontrol of chaos with $F_{2,1}^{P}-1$ works well until the background noise reaches the level of $\sigma \sim 0.1$. Beyond this value, the control loses its effectiveness in retaining LLE close to that of the target state and breakdowns with a noise a little higher. Besides the large external disturbance, the breakdown of the controllability is partly attributed to the strong inherent stability of the fixed-point state, which renders the chaotification difficult.

In the case of further enhancing the chaoticity to $\tilde{\lambda}=1.5$ at a chaotic state of $R=28$, the optimized signal $F_{2,3}^{P}-1$ is of a power $P=5.14\times10^{-3}$. From Fig. 8(b), it is observed that the system at the chaotic state can be further chaotified with the noise level in the range considered and the LLE of the

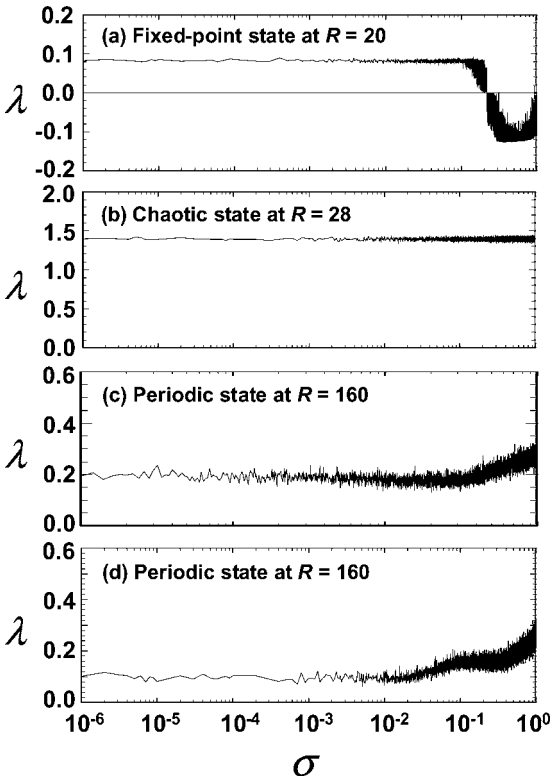

FIG. 8. Effects of background noise on control effectiveness. (a) Signal $F_{2,1}^{P}-1$ (power $P=2.31\times10^{-4}$, target $\tilde{\lambda}=0.1$) applied to fixed-point state at $R=20$; (b) signal $F_{2,3}^{P}-1$ (power $P=5.14\times10^{-3}$, target $\tilde{\lambda}=1.5$) applied to chaotic state at $R=28$; (c) signal $F_{2,2}^{P}-1$ (power $P=1.11\times10^{-6}$, target $\tilde{\lambda}=0.1$) applied to periodic state at $R=160$. (d) Example of improvement in control effectiveness—in the same case of (c), using a GA-optimized signal ($P=1.58\times10^{-6}$) searched under a low-level noise result in an enhanced robustness.

achieved state is approximately 1.4 which deviates a little from the originally expected value of 1.5.

In Fig. 8(c), the case of $R=160$ is taken as an illustrative example of chaotifying a periodic state in the presence of an external disturbance. The GA-optimized signal to chaotify the state to that of $\tilde{\lambda}=0.1$ is $F^P_{2,2}-1$ and is of a power $P=1.11\times10^{-6}$. The chaotification can be reached in the range of σ considered, while the LLE of the target state drifts to a value around 0.2 rather than the original target of 0.1. The deviation from the prescribed LLE of the target due to the presence of the external noise can be reduced using a signal found while considering a small noise. For example, with consideration of a low-level noise, $\sigma=10^{-6}$, a signal of power $P=1.58\times10^{-6}$ ($\omega=18.966\,423\,94$, $\varphi=-2.223\,256\,09$) can be found for the case of periodic state $R=160$. This signal is only of a little higher power, as shown in Fig. 8(d), it performs quite well in achieving the target state of $\tilde{\lambda}=0.1$ even with the noise of $\sigma\sim O(10^{-2})$.

V. CONCLUDING REMARKS

In the present work, we have demonstrated the effectiveness of using very weak periodic and quasiperiodic signals optimized by a GA to chaotify a nonlinear system at either an ordered or a chaotic state. With a preset target LLE for the target state, the control abilities of the present GA-optimized signals in chaos triggering, enhancing and switching control have been demonstrated. Based on the results of these numerical experiments, the following interesting physics about chaotification can be summarized.

(1) In use of periodic signals of high harmonics, the power of the optimized signal is not necessarily reduced with an increasing number of harmonic modes, while using quasiperiodic signals of multiple incommensurable frequencies has the trend of reducing signal power with an increase in the number of the modes. However, the GA-optimized signals of low-mode (2-mode) are favorable for their simplicity and effectiveness.

(2) Although the differences are within one order of magnitude, the power of a quasiperiodic signal needed to reach the control goal is generally lower than a periodic one with the same number of modes.

(3) To destabilize an ordered (fixed-point or periodic) state, the power required for chaotification varies relatively slowly at comparatively lower LLEs but increases drastically as the preset value of the target LLE reaches a certain critical value. Most strikingly, the present numerical experiments demonstrate that this critical value of $\tilde{\lambda}$ corresponds to the LLE of the nearest chaotic state in the neighborhood of the uncontrolled state.

(4) In the case of enhancing the chaoticity of a chaotic state, required control power increases as preset target LLE increases. Unlike that for triggering chaos in ordered states however, there is no obvious slow-varying region appearing in the correlation of minimum power versus target LLE. Performing chaotification with GA-optimized weak perturbations demonstrates that further enhancing the chaoticity of a chaotic state needs more control power than triggering chaos in an ordered state, either fixed-point or periodic state.

(5) Based on the same increment in the system LLE, $\Delta\lambda=\tilde{\lambda}-\lambda_{1,0}$, the control power needed to enhance chaoticity at a chaotic state is higher than that needed to chaotify an ordered state. This fact combined with the above findings (3) and (4) implies that higher power is needed to lead a nonlinear dynamic system to be overchaotified.

(6) In the robustness study, we found that, in general, the GA-optimized signals of minimum power work well even with the condition of strong background noise. In the cases covered in this study, we also found that the LLE of the achieved state may drift a little in the presence of external noise. Nonetheless, this situation can be improved using a signal found by the present GA-based method while considering a small noise. Our test case demonstrated that, although the power increases a little, the signal found by the GA optimization with consideration of a low-level noise is more robust in performing chaotification in a quite noisy environment.

ACKNOWLEDGMENT

The present study was partially supported by the National Science Council of the Republic of China through Grant No. NSC-93-2212-E-035-020.

[1] V. In, M. L. Spano, J. D. Neff, W. L. Ditto, C. S. Daw, K. D. Edwards, and K. Nguyen, Chaos **7**, 605 (1997).
[2] M. P. Kennedy, G. Kolumban, and G. Kis, Int. J. Bifurcation Chaos Appl. Sci. Eng. **10**, 695 (2000).
[3] J. M. Ottino and S. Wiggins, Philos. Trans. R. Soc. London, Ser. A **362**, 923 (2004).
[4] W. Yang, M. Ding, A. J. Mandell, and E. Ott, Phys. Rev. E **51**, 102 (1995).
[5] V. In, S. E. Mahan, W. L. Ditto, and M. L. Spano, Phys. Rev. Lett. **74**, 4420 (1995).
[6] Y. C. Lai and C. Grebogi, Phys. Rev. E **49**, 1094 (1994).
[7] I. B. Schwartz and I. Triandaf, Phys. Rev. Lett. **77**, 4740 (1996).
[8] I. Triandaf and I. B. Schwartz, Phys. Rev. E **62**, 3529 (2000).
[9] V. In, M. L. Spano, and M. Ding, Phys. Rev. Lett. **80**, 700 (1998).
[10] T. Tsubone and T. Saito, IEEE Trans. Circuits Syst., I: Fundam. Theory Appl. **45**, 172 (1998).
[11] T. Tsubone and T. Saito, IEEE Trans. Circuits Syst., I: Fundam. Theory Appl. **45**, 889 (1998).
[12] X. F. Wang and G. Chen, Int. J. Bifurcation Chaos Appl. Sci. Eng. **9**, 1435 (1999).
[13] D. Lai and G. Chen, Int. J. Bifurcation Chaos Appl. Sci. Eng. **13**, 3437 (2003).
[14] S. Codreanu, Chaos, Solitons Fractals **13**, 839 (2002).
[15] X. F. Wang, G. Chen, and X. Yu, Chaos **10**, 771 (2000).

[16] G. Chen, L. Yang, and Z. Liu, IEICE Trans. Fundamentals **E85-A**, 1333 (2002).
[17] K. Konishi, Phys. Lett. A **320**, 200 (2003).
[18] J. Lu, T. Zhou, G. Chen, and X. Yang, Chaos **12**, 344 (2002).
[19] Z. Zheng, J. Lu, G. Chen, T. Zhou, and S. Zhang, Chaos, Solitons Fractals **20**, 277 (2004).
[20] C. Morel, M. Bourcerie, and F. Chapeau-Blondeau, Chaos, Solitons Fractals, **26**, 541 (2005).
[21] H. K. Chen and C. I. Lee, Chaos, Solitons Fractals **21**, 957 (2004).
[22] D. Xu and S. R. Bishop, Phys. Rev. E **54**, 6940 (1996).
[23] Z. M. Ge and T. N. Lin, J. Sound Vib. **259**, 585 (2003).
[24] D. J. Christini and J. J. Collins, Phys. Rev. Lett. **75**, 2782 (1995).
[25] D. J. Christini and J. J. Collins, Phys. Rev. E **52**, 5806 (1995).
[26] S. T. Vohra, L. Fabiny, and F. Bucholtz, Phys. Rev. Lett. **75**, 65 (1995).
[27] R. Chacón, Phys. Rev. Lett. **86**, 1737 (2001).
[28] I. B. Schwartz, I. Triandaf, R. Meucci, and T. W. Carr, Phys. Rev. E **66**, 026213 (2002).
[29] Y. Lei, W. Xu, Y. Xu, and T. Fang, Chaos, Solitons Fractals **21**, 1175 (2004).
[30] Q. S. Li and R. Zhu, Chaos, Solitons Fractals **19**, 195 (2004).
[31] C. Y. Soong, W. T. Huang, F. P. Lin, and P. Y. Tzeng, Phys. Rev. E **70**, 016211 (2004).
[32] C. Y. Soong, W. T. Huang, and F. P. Lin, Chaos, Solitons Fractals (to be published).
[33] A. Wolf, J. B. Swift, H. L. Swinney, and J. A. Vastano, Physica D **16**, 285 (1985).
[34] E. N. Lorenz, J. Atmos. Sci. **20**, 130 (1963).
[35] J. B. Gao, W. W. Tung, and N. Rao, Phys. Rev. Lett. **89**, 254101 (2002).